PASJ: Publ. Astron. Soc. Japan **48**, 1–17 (1996)

Thermal and Chemical Evolution of X-Ray Clusters of Galaxies

Junji FUKUMOTO
Department of Astronomy, Faculty of Science, The University of Tokyo, Bunkyo-ku, Tokyo 113
and
Satoru IKEUCHI
Department of Earth and Space Science, Faculty of Science, Osaka University, Machikaneyama-cho, Toyonaka, Osaka 560

(Received 1995 April 28; accepted 1995 November 28)

Abstract

The thermal and chemical evolution of X-ray clusters of galaxies is explored, pursuing the chemical evolution and gas ejection of member galaxies. We take into account the gas-ejection processes from galaxies to intracluster space by galactic winds powered by supernovae and ram-pressure stripping. The main results are as follows: 1) The metal supply from elliptical galaxies dominates over that of spirals and there is a possibility that ram pressure stripping had occurred at the same or in an earlier epoch than galactic winds in ellipticals. 2) The iron abundance of the intracluster medium (ICM) depends strongly on the initial mass function, but weakly on the star-formation rate of ellipticals, and intermediately on the wind epoch in ellipticals and the cluster richness. 3) The contribution to the ICM from galaxies is much smaller than that of primordial gas.

Key words: Galaxies: abundances — Galaxies: clustering — Galaxies: evolution — Galaxies: formation — Intergalactic medium — X-rays: galaxies

1. Introduction

X-ray satellite observations of clusters of galaxies have revealed high X-ray fluxes, and the temperatures and iron abundances of the intracluster medium (ICM) have been clarified (Jones, Forman 1984; Sarazin 1986; Hughes et al. 1988; Hatsukade 1989; Edge, Stewart 1991a, 1991b; Tsuru 1992). Furthermore, observations have shown that the gas mass is several-times higher than the optical mass of member galaxies, and that the iron abundance is 20–50% of the solar value (Hatsukade 1989; Arnaud et al. 1992). These suggest that most of the ICM is residual primordial gas after galaxy formation (Gunn, Gott 1972), and a sufficient amount of metal-enriched gas has been ejected from member galaxies.

If the iron abundance in galaxies is around the solar value, the total iron mass of the ICM is similar to that of the member galaxies (Renzini et al. 1993). Because observations show the ratio of gas mass to the mass of member galaxies is around 3, the iron abundance of the ICM is around 1/3. The above observations indicate that half of the metal produced in stars has been ejected into intracluster space. Two processes which eject metal-enriched gas from member galaxies into intracluster space have been proposed. One is that when the energy of hot gas heated up by supernova (SN) explosions exceeds the binding energy of a galaxy, the hot gas blows out as a galactic wind (Ikeuchi 1977; Matteucci, Tornambé 1987). The other is that the interstellar gas is stripped out of a galaxy by the ram pressure sweeping of the ICM (Gunn, Gott 1972; Toyama, Ikeuchi 1980; Takeda et al. 1984). Arnaud et al. (1992) studied the correlations between the gas mass, iron mass, and optical luminosity of X-ray clusters of galaxies, and found that the iron mass is directly proportional to the luminosity of elliptical and lenticular galaxies. From this they concluded that only ellipticals and lenticulars have participated in the enrichment of the ICM. On the other hand, Giovanelli and Haynes (1983) found that spiral galaxies in the Virgo core are, on the average, H I deficient by a factor of 2.7 compared with the isolated spirals. This suggests that spirals as well as ellipticals can contribute to the enrichment of the ICM by gas stripping.

Matteucci and Vettolani (1988) and David, Forman, and Jones (1991) studied the evolution of the ICM. But the contribution of the metal and gas mass from spirals has not been taken into account. Himmes and Biermann (1980) examined the case that the ICM is provided by galactic winds in ellipticals and by collisions of galaxies at first; then, gas stripping from spirals also contributes. The iron abundances obtained by these authors are in good agreement with observations. However, we can not

deny the possibility that gas stripping occurs even in ellipticals at very early epochs because the hot gas is greatly concentrated in the center of clusters.

In this paper we examine the chemical evolution of isolated galaxies (both spirals and ellipticals) in the first. Integrating the gas-supply processes from member galaxies by galactic winds and ram pressure stripping, we can study the thermal and chemical evolution of clusters. We specially compare the following cases in order to see which gas-ejection process is most important: (1) galactic wind only, or (2) both galactic winds and stripping. Moreover, we investigate the parameter dependence of the observed quantities.

In section 2 the chemical-evolution model of member galaxies is presented, and in section 3 its numerical results are shown. In section 4, the thermal and chemical evolution of a cluster of galaxies is presented, and in section 5 its numerical results are shown; we also discuss the parameter dependence of the results. In section 6 our primary results are summarized. The symbols of the physical quantities are summarized in the Appendix.

2. Chemical Evolution Model for Galaxies

2.1. *Stellar Data*

The initial mass function (IMF) of stars is usually assumed to be expressed as a power-law form as

$$\phi(m) = (\mu - 1) m_{\rm l}^{\mu-1} m^{-\mu} / [1 - (m_{\rm l}/m_{\rm u})^{\mu-1}], \qquad (1)$$

where $m_{\rm l}$ and $m_{\rm u}$ are the lower and upper stellar mass limits in unit of the solar mass. In the following, we take as $m_{\rm l} = 0.05$ and $m_{\rm u} = 50$. Salpeter (1955) derived $\mu = 1.35$ for the solar neighborhood. Tinsley (1980) found that μ varies from 0.25 to 2.3 for the increasing mass from 0.4 $M_\odot$ to 50 $M_\odot$. The best choice for μ by Arimoto and Yoshii (1987), in order to reproduce the photometric properties of ellipticals, is $\mu = 1.35$. Here, we examine three cases, $\mu = 0.85, 1.35$, and 1.85 for a comparison.

The lifetime of a star with mass m is approximated (Larson 1974) by

$$\log \tau_m = 10.02 - 3.57 \log m + 0.90 \, (\log m)^2. \qquad (2)$$

The fractions of the mass released from a star are as follows (Köppen, Arimoto 1991):

$$\left.\begin{aligned} R(m) &= 0 && \text{for } m \le 0.7, \\ &= 0.42\, m && \text{for } 0.7 < m \le 1.0, \\ &= 1.0 - WD(m)/m && \text{for } 1.0 < m \le 4.8, \\ &= 1.0 - 1.4/m && \text{for } 4.8 < m, \\ WD(m) &= 0.2\, m + 0.43, \end{aligned}\right\} \qquad (3)$$

where $WD(m)$ is the white-dwarf mass from Renzini and Voli (1981).

We consider two types (type Ia and II) of supernovae (SNe). Type Ia SNe come from C-deflagration in white dwarfs in binary systems for $3.0 \le m < 8.0$. Type II SNe come from explosions by a core bounce of single massive stars ($m \ge 8.0$). Matteucci and Tornambé (1987) showed that the fraction of binary systems is around 0.1. We assumed that the iron (^{56}Fe+^{54}Fe) mass ejected from type Ia SN is 0.75 $M_\odot$ following the Nomoto, Thielemann, and Yokoi (1984) model W7. Hillebrandt (1982) found that single stars with $8 \le m \le 12$ experience a core collapse, but the newly synthesized metals remain trapped within remnants, so that there is no contribution to iron enrichment. Tsujimoto (1994) estimated the masses of many kinds of elements ejected from type II SNe for $13 \le m \le 70$. We derived an approximate relation of the ejected iron mass to the SN-progenitor mass based on the above-mentioned results. This iron mass includes ^{54}Fe, ^{57}Fe, ^{58}Fe, and mainly ^{56}Fe. The gas released by a quiet mass loss from red-giant stars is assumed to be the same iron abundance as the interstellar gas at their birth epochs. From the above, the adopted relation of produced iron mass to the stellar mass is as follows :

$$\begin{aligned} R_{\rm Fe}(m) &= \frac{M_{\rm Fe}(t-\tau_m)}{M_{\rm g}(t-\tau_m)} R(m) \quad \text{for } m \le 3.0, \\ &= \frac{0.75}{m} f_{\rm SNI} + \frac{M_{\rm Fe}(t-\tau_m)}{M_{\rm g}(t-\tau_m)} R(m)(1 - f_{\rm SNI}) \\ &\qquad \text{for } 3.0 < m \le 8.0, \\ &= 0 \qquad \text{for } 8.0 < m \le 12.0, \\ &= 1.114/m - 0.104 \\ &\quad + 3.0 \cdot 10^{-3} m - 2.37 \cdot 10^{-5} m^2 \\ &\qquad \text{for } 12.0 < m, \end{aligned} \qquad (4)$$

where $M_{\rm g}(t)$ and $M_{\rm Fe}(t)$ are the gas mass and iron mass in a galaxy, respectively, and $f_{\rm SNI}$ is the fraction of binary systems.

The maximum fraction of binaries is taken as 0.1. The reasons are as follows: Matteucci and Tornambé (1987) adopted the binary fraction $f_{\rm SNI} = 0$ for a model of the chemical evolution of elliptical galaxies, and showed that the predicted current type I SN rate for galaxies is in very good agreement with the observational estimate of Tammann (1974), which is around 0.22 SNe/100 yr/10^{10} $L_\odot$. Thus, if we adopt a larger value than 0.1 as the fraction of binary systems, our models are not consistent with the observations. Moreover, the tendency in current models is more to reduce the influence of SN Ia than to increase it from the observational constraints.

2.2. *Galaxy Model*

We simply assume the one-zone model for a galaxy. That is, a galaxy is a homogeneous sphere, and the star formation and the gas released from stars are averaged as a whole.

2.2.1. *Mass-radius relation*

From the luminosity profile and the line-of-sight velocity dispersion of ellipticals and globular clusters, Saito

(1979) derived a relation between the binding energy, Ω_G, and the total (virial) mass, M_{total}, i.e.,

$$\Omega_G = 5.9 \cdot 10^{58}(M_{total}/10^{11}M_\odot)^{1.45} \text{ erg}. \quad (5)$$

Assuming virial equilibrium, the relation between the total mass and its radius, R_G, is

$$R_G = 7.54(M_{total}/10^{11}M_\odot)^{0.55} \text{ kpc}. \quad (6)$$

As is shown in subsection 3.2, the radius changes at most twice larger than the initial one, because the gas ejection weakens the strength of the gravitational potential. We take equation (6) as the initial radius. Dressler et al. (1987) derived the relation between the velocity dispersion, σ_s, for the stellar motion and the diameter, D_n, estimated from the surface brightness limit ($S_B = 20.75$ mag^{-2}) for Virgo, Fornax, and Comaclusters, i.e.,

$$D_n \propto \sigma_s^{1.333}. \quad (7)$$

Assuming the virial equilibrium and $R_G \propto D_n$,

$$R_G \propto M_{total}^{0.40}. \quad (8)$$

As is shown, the power index to the total mass is less than that in Saito (1979).

Tully and Fisher (1977) pointed out that there is an empirical correlation between the luminosity and the global velocity width, ΔV, for spirals $\Delta V \propto L^{0.4}$. Assuming $M/L =$ constant and $M_{total} \propto \Delta V^2 R_G$, it gives rise to

$$R_G \propto M_{total}^{0.20}. \quad (9)$$

We take the above as the initial radius for spirals. The lower is the mass of a spiral, the more easily is the interstellar gas stripped by the ram pressure, since the power index to the total mass is less than 1/3.

If gas expulsion occurs on a time scale much shorter than the dynamical time scale, the change in the radius of the galaxy by a mass-loss amount of ΔM can be estimated according to Hills (1980):

$$R_G(t_f)/R_G(0) - 1 = \Delta M/[M_{total}(0) - 2\Delta M], \quad (10)$$

where $R_G(0)$ and $M_{total}(0)$ are the initial radius and initial total mass, respectively, and $R_G(t_f)$ is the final radius. From the above, the galaxy can not survive if the amount of mass loss is more than a half of the initial mass. On the contrary, if the gas ejection is much longer than the dynamical time (Mathieu 1983), it becomes

$$R_G(t_f)/R_G(0) - 1 = \Delta M/[M_{total}(0) - \Delta M]. \quad (11)$$

Although in reality the situation is intermediate, we adopt equation (10). We thus overestimate the change of the galaxy radius.

2.2.2. Mass-luminosity relation

While the mass-to-luminosity ratio for galaxies of the same morphological type is dispersed, we assume that the average value for sprirals and ellipticals are $M_{total}/L_B = 6M_\odot/L_{B_\odot}$ and $M_{total}/L_B = 12M_\odot/L_{B_\odot}$, respectively (Faber, Gallagher 1979; Binney, Tremaine 1987; Trimble 1987), because clusters of galaxies have many galaxies. The galaxy mass, M_G, is defined as the sum of stellar and gas masses. Since the total (virial) mass-to-galaxy mass ratio, M_{total}/M_G, is independent of the morphology for spirals (Faber, Gallagher 1979; Larson, Tinsley 1978), we assume $M_{total}(0)/M_G(0) = 2$ as the initial value. However, since in the outer layer the mass-to-luminosity ratio is much larger, the occurrence of galactic winds is unpredictable because of the dependence on the total mass. Moreover, there is a possibility that gas is gradually released from outward, because of the shallowness of the potential well. We take the epoch of the galactic wind as a parameter, though a plausible value is estimated.

2.2.3. Star formation rate

For the sake of simplicity, as a reasonable assumption we have chosen a star-formation rate proportional to some power of the gas density (Schmidt 1959):

$$F(t) = \alpha[M_g(t)/M_g(0)]^{k-1}M_g(t), \quad (12)$$

where α is a constant, and is expressed in units of (10 Gyr)$^{-1}$. Two observations, i.e., the gas fraction in a galaxy and the metal abundance in the interstellar gas, determine α. Madore (1977) derived $k = 1/2$ by comparing the results of numerical simulations with the correlation between the gas density and the density of H II regions or bright stars. The $k = 2$ case has been suggested assuming star formation induced by cloud-cloud collisions. For a comparison, we studied for three cases, $k = 1/2, 1$, and 2.

Taking into account the stellar lifetime, the gas and iron mass released from red giant stars and SNe per unit time are respectively given as follows:

$$G(t) = \int_{m_l}^{m_u} F(t - \tau_m)\phi(m)R(m)dm, \quad (13)$$

$$G_{Fe}(t) = \int_{m_l}^{m_u} F(t - \tau_m)\phi(m)R_{Fe}(m)dm. \quad (14)$$

2.3. Galactic Wind

As soon as the gas temperature exceeds 10^4 K, the radiative cooling becomes rather efficient, as $\Gamma_{cool}/n_g^2 \sim 10^{-22}$erg cm^3 s^{-1} (Cox, Tucker 1969), where Γ_{cool} and n_g is the cooling function and the number density of the interstellar gas, respectively. We define the heating function as the energy-supply rate by SNe per unit time per

unit volume. Assuming the instantaneous recycling approximation for $m \geq 3$ and locked-up for $m < 3$, the heating function is given by

$$\Gamma_{\rm heat} = \frac{e_{\rm SN}}{4\pi R_{\rm G}^3/3}\alpha[M_{\rm g}/M_{\rm g}(0)]^{k-1}M_{\rm g}, \tag{15}$$

$$e_{\rm SN} = \int_3^{m_{\rm u}} \phi(m)\varepsilon_{\rm SN}/m\, dm, \tag{16}$$

where $e_{\rm SN}$ and $\varepsilon_{\rm SN}$ are the energy supplied by SNe per unit mass and the kinetic energy released from an SN, respectively. Assuming $\varepsilon_{\rm SN} = 10^{51}$ erg, the ratio of the cooling time, $t_{\rm cool}$, to the heating time, $t_{\rm heat}$, is expressed as :

$$\begin{aligned}\frac{t_{\rm cool}}{t_{\rm heat}} &= \frac{\Gamma_{\rm heat}}{\Gamma_{\rm cool}} \\ &= 0.7\left(\frac{\alpha}{100}\right)\left(\frac{e_{\rm SN}}{10^{16}{\rm erg\ g^{-1}}}\right)\left[\frac{M_{\rm g}}{M_{\rm g}(0)}\right]^{k-1} \\ &\quad\times\left(\frac{M_{\rm g}}{10^{11}M_\odot}\right)^{-1}\left(\frac{R_{\rm G}}{7.54\ {\rm kpc}}\right)^3,\end{aligned} \tag{17}$$

where $e_{\rm SN}$ (in erg g^{-1}) depends upon the power index of IMF, μ, as $e_{\rm SN}$ to be 10^{16}, 4×10^{15}, and 6×10^{14} for $\mu =$ 0.85, 1.35, and 1.85, respectively. For $R_{\rm G} = 10$ kpc and $M_{\rm g} = 10^{11}M_\odot$, which are reasonable initial conditions, cooling processes dominate at an early epoch in the case $\alpha < 1000$. The cooling processes gradually become inefficient along with a decrease in the gas density. Soon, the heating processes dominate and a galactic wind occurs when the thermal energy of the gas exceeds the binding energy of the gas. The upper limit for α (<1000) is consistent with a model which reproduces the photometric data of ellipticals by Arimoto and Yoshii (1987). The epoch in which the galactic wind occurs, $t_{\rm w}$, is roughly estimated as $t_{\rm w} = 10^7$ yr for $\alpha = 10^3$ and $\mu = 0.85$ to $t_{\rm w} = 10^8$ yr for $\alpha = 50$ and $\mu = 1.85$. However, their model has not taken account of any dark-matter component. David, Forman, and Jones (1990) and Ciotti et al. (1991) solved the time-dependent, Eulerian equations of gasdynamics with source terms. They took account of the massive dark halo estimated by using the central-velocity dispersion of stars, and assuming its mass-to-luminosity ratio to be around 10. On the other hand, Forman, Jones, and Tucker (1985) showed that mass-to-luminosity ratios estimated by using the temperature of the X-ray gas are larger, ranging from 10 to 80. Arimoto and Yoshii (1987) suggested that if the interstellar gas is much hotter, the efficiency of star formation is considerably reduced, so that the wind epoch becomes later. From these studies, the wind epoch cannot be determined exactly. Thus, we take this time $t_{\rm w}$ as a parameter in the above estimated ranges. We assume that the interstellar gas escapes from the surface of a galaxy at its sound velocity. Then, the gas-escape rate is

Table 1. Spiral galaxy model.

α (10 Gyr)$^{-1}$	μ	k	$f_{\rm SNI}$	$M_{\rm g}/M_{\rm G}$	$Z_{\rm Fe}$ ($Z_{\rm Fe_\odot}$)	$M_{\rm Fe}/M_{\rm G}$ (10^{-4})
1.0	1.35	1	0.1	0.30	1.3	6.5
0.3	1.35	1	0.1	0.70	0.41	4.7
3.0	1.35	1	0.1	0.034	3.1	1.8
1.0	0.85	1	0.1	0.51	2.7	23
1.0	1.85	1	0.1	0.24	0.30	1.2
1.0	1.35	1/2	0.1	0.16	1.9	5.0
1.0	1.35	2	0.1	0.46	0.88	6.6
1.0	1.35	1	0.0	0.30	0.25	1.3
1.0	1.35	1	0.05	0.30	0.78	3.9

$$\begin{aligned} W(t) &= 0 \qquad\quad \text{for } t < t_{\rm w} \\ &= 4\pi R_{\rm G}^2\rho_{\rm g}c_{\rm s} \text{ for } t \geq t_{\rm w},\end{aligned} \tag{18}$$

where $c_{\rm s}$ and $\rho_{\rm g}$ are the sound velocity and the interstellar gas density, respectively, and $t_{\rm w}$ is expressed in units of Gyr.

2.4. *Basic Equations*

From the above considerations, the evolutions of the stellar mass, $M_{\rm s}$, gas mass, $M_{\rm g}$, and iron mass, $M_{\rm Fe}$, in a galaxy are given, respectively, by

$$\frac{dM_{\rm s}(t)}{dt} = F(t) - G(t), \tag{19}$$

$$\frac{dM_{\rm g}(t)}{dt} = -F(t) + G(t) - W(t), \tag{20}$$

$$\frac{dM_{\rm Fe}(t)}{dt} = -Z_{\rm Fe}(t)F(t) + G_{\rm Fe}(t) - Z_{\rm Fe}(t)W(t), \tag{21}$$

where $Z_{\rm Fe}$ is the iron abundance, $Z_{\rm Fe}(t) = M_{\rm Fe}(t)/M_{\rm g}(t)$. Thus, a galaxy mass, which is the sum of stellar and gas masses, $M_{\rm G}$, changes as

$$\frac{dM_{\rm G}(t)}{dt} = -W(t). \tag{22}$$

This means that the decrease in the galaxy mass depends only upon the galactic wind. We adopt $M_{\rm s}(0) =$ 0, $M_{\rm g}(0) = M_0$, $M_{\rm Fe}(0) = 0$, and $M_{\rm G}(0) = M_0$ as reasonable initial conditions. Regarding the ram-pressure stripping, we discuss this situation in subsection 4.1 seperately.

The evolution of the energy of interstellar gas, $E_{\rm g}$, is given by

$$\begin{aligned}\frac{dE_{\rm g}(t)}{dt} &= \int_{m_{\rm l}}^{m_{\rm u}} F(t-\tau_m)\phi(m)\varepsilon_{\rm SN}/m\, dm \\ &\quad + \frac{1}{2}G(t)V_{\rm ML}^2 - \frac{3}{2}[F(t)+W(t)]\,c_{\rm s}^2,\end{aligned} \tag{23}$$

where $V_{\rm ML}$ is the gas velocity released from a star by quiet mass-loss processes, and we take $V_{\rm ML} = 100$ km s^{-1}.

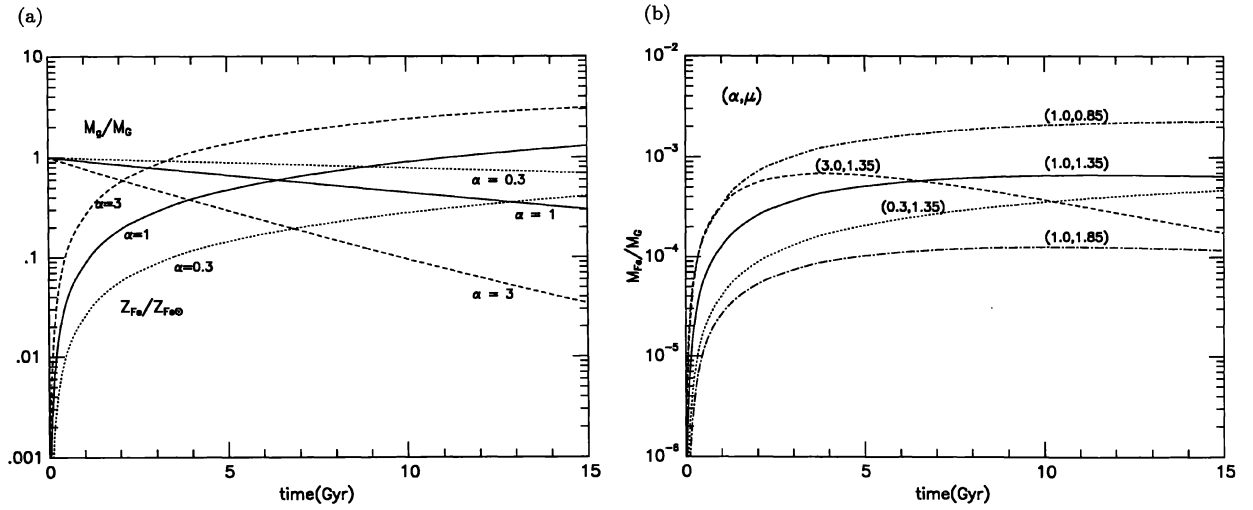

Fig. 1. (a) Evolution of the mass ratio of interstellar gas to that of a galaxy, M_g/M_G; the iron abundance of the interstellar gas in a spiral, $Z_{Fe}/Z_{Fe_\odot}$, is shown for three cases: $\alpha = 0.3$ (dotted curve), 1 (solid curve), and 3 (dashed curve) with $\mu = 1.35$ and $k = 1$. (b) Evolution of the mass ratio of iron in interstellar gas to that of a galaxy, M_{Fe}/M_G, in a spiral shown for five cases: $(\alpha, \mu) = (0.3, 1.35)$ (dotted curve), (1.0, 1.35) (solid curve), (3.0, 1.35) (dash curve), (1.0, 0.85) (dot-short dash curve), and (1.0, 1.85) (dot-long dash curve) with $k = 1$.

3. Numerical Results for Galaxy Evolution

In this section we summarize the dependence of galaxy evolution on several parameters for isolated galaxies (both spirals and ellipticals), and get the best-fit values to be consistent with observations for the basic evolution models, which are the bases for calculating finally the evolution of X-ray clusters of galaxies. The adopted parameters and numerical results are summarized in table 1 and figure 1 for spirals and in tables 2 and 3 and figure 2 for ellipticals.

3.1. Spiral Galaxy

The columns in table 1 are as follows: From the 1st to 4th columns are the adopted parameters as the star-formation coefficient, α, the power index of the IMF, μ, the power index of the star-formation rate, k, and the fraction of binary systems, f_{SNI}. From the 5th to 7th are the calculated results at $t = 15$ Gyr as the gas mass-to-galaxy mass ratio, M_g/M_G, the iron abundance, Z_{Fe}, and the iron mass-to-galaxy mass ratio, M_{Fe}/M_G.

We adopt $Z_{Fe_\odot} = 1.64 \times 10^{-3}$ as the iron abundance for the solar value (Allen 1973). In the parameter ranges searched in the present calculations, galactic winds are not necessary to take into account for spirals, because from equation (17) it holds $t_{cool}/t_{heat} \simeq 10^{-3} \ll 1$ for all models, that is, cooling by the rich-gas density is always efficient. Therefore, M_G does not change in time. For the dependence of the gas fraction and the metallicity on α and μ, our results are essentially the same as those of Arimoto and Yoshii (1986). Their star-formation coefficient, $\alpha_{AY} = 1$, corresponds to $\alpha = 1.9$ in our unit.

To see the dependence on a star-formation coefficient, the evolution of the gas fraction to the galaxy mass, M_g/M_G, and the iron abundance, $Z_{Fe}/Z_{Fe_\odot}$, in a spiral for three cases, $\alpha = 0.3$ (dotted curve), 1.0 (solid curve), and 3.0 (dashed curve) are shown in figure 1a for the case with $k = 1$ and $\mu = 1.35$. As can be seen, the gas mass and iron abundance change rapidly with increasing α, which characterizes the time scale of the galactic evolution. In these parameters, $\alpha = 1.0$ is in good agreement with the observations, such as $0.05 \leq M_g/M_G \leq 0.5$ (Young, Scoville 1991), and $0.4 \leq Z_{Fe}/Z_{Fe_\odot} \leq 4$ (Pagel, Edmunds 1981).

To determine the dependence of the iron abundance on the star formation coefficient and the power index of the IMF, the evolutions of the ratio of the iron mass to the initial galaxy mass for five cases, $(\alpha, \mu) = (0.3, 1.35)$ (dotted curve), $(\alpha, \mu) = (1.0, 1.35)$ (solid curve), $(\alpha, \mu) = (3.0, 1.35)$ (dash curve), $(\alpha, \mu) = (1.0, 0.85)$ (dot-short dash curve), $(\alpha, \mu) = (1.0, 1.85)$ (dot-long dash curve) for k=1 are shown in figure 1b. The best two-parameter (α, μ) set consistent with observations is the case for (1.0, 1.35), because if the star-formation coefficient is larger, the gas fraction decreases and the iron abundance increases. On the contrary, if the power of the IMF is steeper, both decrease (see table 1). The reason for this tendency is easily understood in that the star-formation

Table 2. Elliptical galaxy model I.

α $(10\ \mathrm{Gyr})^{-1}$	μ $(10^{10}M_\odot)$	t_w (Gyr)	k	$M_G(0)$ $(10^{10}M_\odot)$	f_{SNI}	M_g (wind) $(10^{10}M_\odot)$	M_g/M_G (10^{-5})	Z_{Fe} $(Z_{Fe_\odot})$	R_G $(R_G(0))$	M_G $(10^{10}M_\odot)$	M_g^E $(10^{10}M_\odot)$	M_{Fe}^E $(10^7M_\odot)$	Z_{Fe}^E $(Z_{Fe_\odot})$
100	1.35	0.5	1	10	0.1	0.21	2.0	1.0	1.0	9.1	0.86	4.1	2.9
30	1.35	0.5	1	10	0.1	2.72	3.4	0.51	1.2	6.9	3.1	8.7	1.7
300	1.35	0.5	1	10	0.1	0.023	1.3	1.3	1.0	9.4	0.57	1.6	1.7
100	0.85	0.5	1	10	0.1	0.83	2.5	2.4	1.1	7.7	2.3	21	5.5
100	1.85	0.5	1	10	0.1	0.088	1.3	0.24	1.0	9.7	0.28	1.2	0.86
100	1.35	0.1	1	10	0.1	4.0	2.3	0.37	1.3	5.9	4.1	11	1.6
100	1.35	1.0	1	10	0.1	0.040	2.0	1.2	1.0	9.4	0.55	1.4	1.6
100	1.35	0.5	1/2	10	0.1	2.0	9.0	0.51	1.2	7.5	2.5	8.6	2.1
100	1.35	0.5	2	10	0.1	0.002	1.3	1.3	1.0	9.5	0.46	1.3	1.7
100	1.35	0.5	1	1	0.1	0.013	1.2	0.91	1.1	0.91	0.094	0.43	2.8
100	1.35	0.5	1	100	0.1	2.7	4.2	1.2	1.0	93.0	7.3	36	3.0
100	1.35	0.5	1	10	0.0	0.21	2.1	0.27	1.0	9.2	0.84	0.54	0.39
100	1.35	0.5	1	10	0.05	0.21	2.0	0.66	1.0	9.2	0.85	2.3	1.6

Table 3. Elliptical galaxy model II.

α $(10\ \mathrm{Gyr})^{-1}$	μ $(10^{10}M_\odot)$	t_w (Gyr)	k	$M_G(0)$ $(10^{10}M_\odot)$	f_{SNI}	M_g (wind) $(10^{10}M_\odot)$	M_g/M_G (10^{-5})	Z_{Fe} $(Z_{Fe_\odot})$	R_G $(R_G(0))$	M_G $(10^{10}M_\odot)$	M_g^E $(10^{10}M_\odot)$	M_{Fe}^E $(10^7M_\odot)$	Z_{Fe}^E $(Z_{Fe_\odot})$
30	0.85	0.5	1	10	0.1	4.3	4.4	1.3	1.5	4.8	5.2	27	3.2
30	1.35	1.0	1	10	0.1	0.83	3.1	0.85	1.1	8.6	1.4	5.3	2.4
100	0.85	0.1	1	10	0.1	5.4	3.6	1.0	2.0	3.6	6.4	31	2.9
100	1.35	0.5	1	10	0.1	0.21	2.0	1.0	1.0	9.1	0.86	4.1	2.9
100	1.35	1.0	1	10	0.1	0.040	2.0	1.2	1.0	9.4	0.55	1.4	1.6
300	1.35	0.5	1	10	0.1	0.023	1.3	1.3	1.0	9.4	0.57	1.6	1.7

coefficient determines the gas fraction, and the power index of the IMF determines the fraction of locked-up mass to the mass of stars which release heavy elements. As can be seen in table 1, the gas fraction and the metallicity depend weakly on k compared with the other parameters. As is easily seen, the iron mass depends sensitively on the power index of the IMF, as is expected from the above considerations. Since the iron mass is almost independent of k from table 1, only the power index of the IMF mainly affects the iron abundance in a spiral. Since the iron mass is nearly constant after 5 Gyr for $\alpha = 1$, the contribution to the iron abundance of the ICM is the same at any time if stripping occurs after this time. Thus, the amount of iron ejected from a spiral is nearly proportional to the initial spiral mass.

From the above results, we fix $(\alpha, \mu, k) = (1.0, 1.35, 1)$ for spirals for the basic model in the calculation of the thermal and chemical evolution of X-ray clusters of galaxies.

3.2. *Elliptical Galaxy*

The columns in tables 2 and 3 are as follows: From the 1st to 7th are the adopted parameters as the star-formation coefficient, α, the power index of the IMF, μ, the time when the galactic wind occurs, t_w, the power index of the star-formation rate, k, the initial elliptical mass, $M_G(0)$, the fraction of binary systems, f_{SNI}, and the interstellar gas mass at the galactic wind, M_g(wind). From 8th to 14th are the calculated results at t=15 Gyr as the gas mass-to-galaxy mass ratio, M_g/M_G, the iron abundance, Z_{Fe}, the final radius, R_G, the elliptical mass, M_G, the total gas mass ejected from an elliptical, M_g^E, the total iron mass ejected from an elliptical, M_{Fe}^E, and the average iron abundance for the ejected gas, Z_{Fe}^E.

The time when the galactic wind occurs was studied for three cases, $t_w = 0.01, 0.05$, and 0.1, as is suggested by Arimoto and Yoshii (1987) and Matteucci and Tornambé (1987).

As can be seen in table 2, the ratio of interstellar gas to the galaxy mass is less than 10^{-4} in any case. Since Forman, Jones, and Tucker (1985) showed that ellipticals

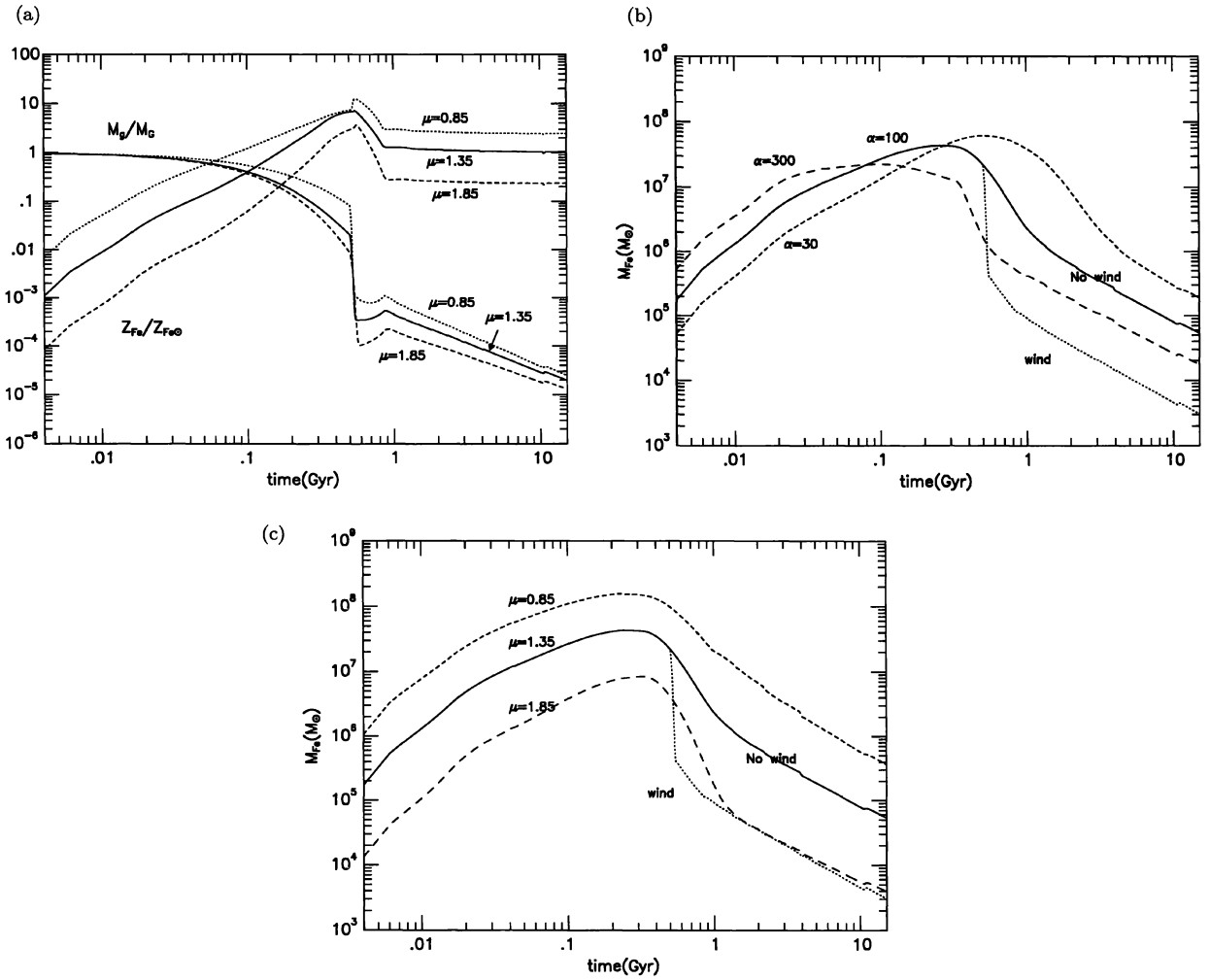

Fig. 2. (a) Evolution of the mass ratio of the interstellar gas to galaxy, $M_g(t)/M_G$, and the iron abundance of the interstellar gas in an elliptical, $Z_{Fe}/Z_{Fe_\odot}$, is shown for three cases, $\mu = 0.85$ (dotted curve), 1.35 (solid curve), and 1.85 (dashed curve) with $\alpha = 100$ and $k = 1$. (b) Evolution of the iron mass, M_{Fe}, in interstellar gas without a galactic wind in an elliptical shown for three cases: $\alpha = 30$ (dashed curve), 100 (solid curve), and 300 (long-dashed curve) with $\mu = 1.35$ and $k = 1$. The effect of a galactic wind starting at $t_w = 0.5$ Gyr is shown for the case $\alpha = 100$ (dotted curve). (c) Evolution of the iron mass, M_{Fe}, in interstellar gas without a galactic wind in an elliptical is shown for three cases, $\mu = 0.85$ (dashed curve), 1.35 (solid curve), and 1.85 (long-dashed curve) with fixing $\alpha = 100$ and $k = 1$. The effect of a galactic wind starting at $t_w = 0.5$ Gyr is shown for the case $\mu = 1.35$ (dotted curve).

generally have a considerable amount of hot interstellar gas, the interstellar gas estimated by us does not agree with the observations. However, we suppose that the interstellar gas of ellipticals at present comprises two components. One is cold and/or warm gas which is released from stars; we calculated this component as the interstellar gas. Even if all of this gas becomes HI, our results satisfy the observed upper limit of HI gas (Gallagher, Faber, Balick 1976). The other is hot gas, and a part of this component released by the galactic wind remains around the galaxy. We ignored this hot gas. Forman, Jones, and Tucker (1985) showed that the mass ratio of observed hot gas to stars is from 0.001 to 0.07. On the other hand, Matteucci and Tornambé (1987) showed that the mass ratio of hot gas released from an elliptical galaxy by the galactic wind to stars is around 0.1. From the above, most of released gas spreads into the intracluster space. Thus, we can ignore the observed hot gas.

The iron abundance of interstellar gas depends upon several parameters, and the observed iron abundance in stars ($0.4 \leq Z_{Fe}/Z_{Fe_\odot} \leq 1.5$, Pagel, Edmunds 1981) gives

constraints on the input parameters. As can be seen, the case $(\alpha, k) = (100, 1/2)$ gives similar results as in the case $(\alpha, k) = (300, 1)$. Since the star-formation rate is determined by two parameters (k and α), as given in equation (12), the resultant evolutionary behavior of the star-formation rates for the above two cases are alike. From now on, for simplicity with fixing $k = 1$, we examine the evolution by varying α for the star-formation rate.

The ejected gas per unit time at the time when the galactic wind occurs is estimated by using equations (6) and (18) as

$$W(t_w) \propto R_G(0)^2 \rho_g \propto R_G(0)^{-1} M_g \propto M_{total}^{-0.55} M_g. \quad (24)$$

Until the galactic-wind epoch, all quantities of an elliptical galaxy evolve in proportion to the initial total mass. From the above equation, the gas-ejection rate is proportional to the gas mass, not to the total mass. Thus, all of the gas mass ejected by the galactic wind is not proportional to the total mass. This is understood because the surface area per unit gas mass is smaller for the larger total mass. However, the difference is very small (see table 2). If equation (8) is adopted as the relation of the total mass to its radius the difference described above becomes much smaller. Thus, the difference in the total masses has little effect on the gas supply to the ICM.

As table 2 shows, the iron abundance of the interstellar gas, the total ejected gas mass, M_g^E, and the total ejected iron mass, M_{Fe}^E, depend strongly upon the power index of the IMF; the parameter which affects the evolution of the ICM most effectively is the power index of the IMF in ellipticals. The cases for $f_{SNI} \leq 0.05$, and/or $\mu = 1.85$ are not in agreement with the observations. From now on, we discuss the case $f_{SNI} = 1$, and $\mu = 0.85$ or 1.35.

The average iron abundance ejected from an elliptical has the maximum value for the case $\alpha = 100$ among three cases, $\alpha = 30$, 100, and 300. The reasons are as follows: For reference, we examine the time variation of the iron abundance in interstellar gas for the case when a galactic wind does not occur. In an early stage, gases are released from red-giant stars and SNe, and the iron abundance in the interstellar medium gradually increases. Soon, the iron abundance reaches to the maximum, and then decreases because metal-poor gas begins to be released from low-mass stars. The star-formation rate determines when the iron abundance becomes maximum. When α is less than 100, the star formation is not so active that the increase of iron is delayed and the galactic wind occurs before the peak epoch. If α is larger than 100, since the galactic wind occurs after the peak epoch, Z_{Fe}^E is small. If α is nearly 100, the galactic-wind epoch is almost the same as the peak one. Therefore, Z_{Fe}^E is the maximum for $\alpha \sim 100$.

On the other hand, the average gas mass ejected from an elliptical galaxy decreases with increasing the star-formation rate. The reasons are as follows: In an early epoch, since the life time of almost all low-mass stars formed in very early epochs is longer than this age of the elliptical galaxy, the gas mass released from stars is much smaller than the interstellar one. Therefore, the gas mass decreases due to the star formation. Since the galactic wind ejects most of the interstellar gas into the intracluster gas, the ejected gas mass is almost the same as the mass of the interstellar gas, M_g(wind). Therefore, the ejected gas mass at the galactic-wind epoch also decreases with increasing the star-formation rate, as can be seen in table 2. Even if the gas which is continuously released from the low-mass stars contributes much to the interstellar gas at the galactic-wind epoch, the total ejected gas mass decreases with increasing star-formation rate, because the gas mass at the galactic-wind epoch strongly depends on the star-formation rate. Note that these discussions are based on a fixed galactic-wind epoch. This assumption is not correct. The reasons are as follows: the binding energy of this galaxy is independent of the star-formation rate, while the thermal energy of this gas strongly depends on the star-formation rate. Hence, for a larger star-formation rate the gas would be ejected, while for a lower star formation rate it would remain binded to the galaxy. Consequently, it is expected that the larger is the star-formation rate, the shorter is the galactic-wind epoch and the larger is the ejected gas mass. Although the galactic-wind epoch is not independent of the star-formation rate, we treat these as independent parameters in order to investigate the effects of each parameter.

In figure 2a, we show the evolutions of M_g/M_G and $Z_{Fe}/Z_{Fe_\odot}$ for three cases, $\mu = 0.85$, 1.35, and 1.85. As soon as a galactic wind occurs, the interstellar gas decreases rapidly. Thus M_g/M_G decreases similarly because the amount of the interstellar gas is much smaller than that of the galaxy mass. As a result, newly born stars from the interstellar gas decrease. The interstellar gas is affected by two gas components from the low-mass stars with low iron abundances and from the intermediate and massive stars with high iron abundances. After 0.4 Gyr from the galactic-wind epoch, which corresponds to the lifetime of stars for type Ia SNe, the iron abundance Z_{Fe} becomes nearly constant for any cases. In other words, the galactic-wind epoch is just the epoch when Z_{Fe} reaches its maximum, as can be easily seen by comparing Z_{Fe}^E with $Z_{Fe}(t = 15$ Gyr) in table 2. For all cases, Z_{Fe}^E is larger than $Z_{Fe_\odot}$ (see the same table), and the iron abundance of the ICM is 3-times more than the observed one, if the primordial gas is absent. Moreover, the ejected gas mass is much smaller than the initial mass. These two results strongly indicate the necessity of the primordial gas for the ICM.

At an early epoch ($t < 0.01$ Gyr), the large amount of gas produces many massive stars as the progenitors of type Ia and II SNe. Since the iron mass supplied into the interstellar gas by those stars is much larger than

that locked into the newly born stars, the iron mass increases rapidly, as shown in figures 2b and 2c. After $t = 0.1$–0.5 Gyr, the amount of the iron in the interstellar gas reaches to the maximum, and then decreases rapidly. Therefore, the ejected iron mass depends strongly on the galactic-wind epoch.

We next examine sets of parameters consistent with the observations. While the set of parameters in spirals is fixed uniquely, in ellipticals the parameter sets can not be fixed by using two observations, the upper limit for the amount of the interstellar gas and the iron abundance. We present the results for the six models of different parameters in table 3. As can be seen in table 3, the iron abundances $Z_{\rm Fe}^{\rm E}$, ejected into the intracluster space in six models are not so different compared with those of the ejected iron masses, $M_{\rm Fe}^{\rm E}$. Therefore, the amount of primordial gas has great influence on the iron abundance in the intracluster gas. From now on, we discuss these six models for ellipticals.

4. Chemical Evolution Model of X-Ray Clusters of Galaxies

The neutral hydrogen masses of cluster spirals have been compared with those of a similar sample of isolated galaxies. Giovanelli and Haynes (1983) found that the spirals in the Virgo core are, on the average, H I deficient by a factor of 2.7 with respect to isolated spirals. Sullivan and Johnson (1978) also showed that the A1367 and the Coma (A1656) spirals have lower values of neutral hydrogen masses than isolated spirals by a factor of at least 4, though the Coma value is probably most extreme. These observations suggest that the process responsible for removing the interstellar gas from spirals is ram-pressure stripping by the ICM. Further, these observations suggest that at an early epoch the ram-pressure stripping would also occur in gas-rich ellipticals. Thus, we calculate the evolution of a cluster of galaxies while taking into accont the ram-pressure stripping from spiral and elliptical galaxies.

4.1. Basic Equations with Gas Stripping

The interstellar gas in a galaxy moving through the ICM with velocity, $\sigma_{\rm G}$, is subject to the ram pressure and is stripped from the galaxy if a sufficient amount of momentum is transferred. A simple criterion of the stripping is given as (Gunn, Gott 1972)

$$\rho_{\rm c}\sigma_{\rm G}^2 > \gamma\rho_{\rm g}\sigma_{\rm s}^2, \tag{25}$$

where $\rho_{\rm g}$ and $\rho_{\rm c}$ are the interstellar gas density and the ICM density, respectively, and $\sigma_{\rm s}^2 (= GM_{\rm total}/R_{\rm G})$ is the random velocity of stars in a galaxy. The numerical factor γ depends on the galaxy structure, and its value may vary from $\sim 10^{-2}$ in a flat galaxy to ~ 10 in a centrally condensed spherical galaxy (Takahara, Ikeuchi 1977). We take the gas-stripping time while the ICM passes through the galaxy. Thus, the gas-stripping rate is assumed to be

$$S(t) = \frac{\sqrt{3}\sigma_{\rm s}M_{\rm g}}{R_{\rm G}}\sqrt{\frac{\rho_{\rm c}\sigma_{\rm G}^2}{\rho_{\rm g}\sigma_{\rm s}^2} - \gamma}. \tag{26}$$

Though this criterion seems to be out of date, a two-dimensional simulation of mass stripping by Murakami and Ikeuchi (1994) recently showed almost the same results. That is, when the central pressure is lower than the ram pressure of a supersonic wind, the gas cloud is blown out from the potential of the matter with a time scale corresponding to the wind crossing time of the cloud. Thus, we do not think that the treatment of the stripping is out of date.

Then, basic equations (19), (20), and (21) for a galaxy are changed to

$$\frac{dM_{\rm g}(t)}{dt} = -F(t) + G(t) - W(t) - S(t), \tag{27}$$

$$\frac{dM_{\rm Fe}(t)}{dt} = -Z_{\rm Fe}(t)F(t) + G_{\rm Fe}(t) - Z_{\rm Fe}(t)W(t) - Z_{\rm Fe}(t)S(t). \tag{28}$$

The galaxy mass follows,

$$\frac{dM_{\rm G}(t)}{dt} = -W(t) - S(t). \tag{29}$$

We take the initial conditions to be the same as in subsection 2.4. The evolution of the energy of the interstellar gas is given by

$$\frac{dE_{\rm g}(t)}{dt} = \int_{m_{\rm l}}^{m_{\rm u}} F(t-\tau_m)\phi(m)\varepsilon_{\rm SN}/m\, dm + \frac{1}{2}G(t)V_{\rm ML}^2 - \frac{3}{2}[F(t) + W(t) + S(t)]\, c_{\rm s}^2. \tag{30}$$

4.2. Model and Basic Equations for Clusters of Galaxies

We consider the cluster to be a closed system for the mass. In other words we assume that intracluster gas is not released from the cluster. Its structure is assumed to be a one-zone sphere like a model galaxy.

The basic equations of the evolutions for the total mass of member galaxies, $M_{\rm G}^{\rm c}$, and the mass of the ICM, $M_{\rm g}^{\rm c}$, are as follows:

$$\frac{dM_{\rm G}^{\rm c}(t)}{dt} = \int_{M_{\rm G}^{\rm l}}^{M_{\rm G}^{\rm u}} n(M_0)\frac{dM_{\rm G}(M_0,t)}{dt}dM_0, \tag{31}$$

$$\frac{dM_{\rm g}^{\rm c}(t)}{dt} = -\frac{dM_{\rm G}^{\rm c}(t)}{dt}, \tag{32}$$

Table 4. Summary of observations of X-ray clusters (Arnaud et al. 1992).

Cluster name	$M_{\rm G}^{\rm c}$ ($10^{13}M_\odot$)	$M_{\rm g}^{\rm c}$ ($10^{13}M_\odot$)	$M_{\rm Fe}^{\rm c}$ ($10^{10}M_\odot$)	$M_{\rm g}^{\rm c}/M_{\rm G}^{\rm c}$	$Z_{\rm Fe}^{\rm c}$ ($Z_{\rm Fe_\odot}$)	$L_{\rm X}$ (10^{45} erg s^{-1})	$T_{\rm g}$ (keV)
Virgo	0.881	0.636	0.627	0.722	0.44	0.020	2.34
A1367	1.24	3.31	2.30	2.67	0.31	0.091	3.50
A2199	2.29	3.82	3.85	1.67	0.21	0.297	4.71
A1795	1.98*	10.7	8.63	5.40	0.36	1.06	5.34
A426	4.18	7.63	5.64	1.83	0.33	1.29	6.08
A2256	3.96	9.29	5.83	2.35	0.28	1.11	7.51
A1656	4.30	6.87	3.39	1.60	0.22	0.817	8.11
A2142	3.71*	8.90	5.58	2.40	0.28	2.91	8.68

* This value is derived from Tsuru (1992).

where M_0 refers to $M_{\rm G}(0)$, and $n(M_0)$ is the initial-mass function for galaxies. We take the lower and upper mass limits of member galaxies in the initial epoch as $M_{\rm G}^{\rm l} = 10^{10}\ M_\odot$ and $M_{\rm G}^{\rm u} = 10^{12}\ M_\odot$, respectively.

The notation c means the quantity of a cluster. We adopt the initial-mass function for galaxies estimated from the luminosity function of the Virgo cluster (Sandage 1990) by using mass-to-luminosity ratios as in subsection 2.2, i.e., $M_{\rm G}/L_B = 3\ M_\odot/L_{B_\odot}$ for spirals and $M_{\rm G}/L_B = 6\ M_\odot/L_{B_\odot}$ for ellipticals. This function is expressed as

$$n(M_0) \propto \exp\left[-\left(\frac{\log M_0 + a}{b}\right)^2\right]. \tag{33}$$

We adopt $(a,b) = (1.03, 0.8)$ for spirals and $(a,b) = (0.72, 1.2)$ for ellipticals because the variances of the observed mass functions for spirals and ellipticals are 2 and 3 magnitudes, respectively, and these peaks are -19 magnitudes for both galaxies. The coefficient of those functions is determined by the number ratios of ellipticals to spirals ($N_{\rm E}/N_{\rm S}$) and all initial galaxy mass $M_{\rm G}^{\rm c}(0)$.

The evolution of the energy of the ICM is given by

$$\frac{dE_{\rm g}^{\rm c}(t)}{dt} = E_{\rm s}(t) + E_{\rm w}(t) - L_{\rm X}(t), \tag{34}$$

$$E_{\rm s}(t) = \int n(M_0)\frac{3}{2}S_{M_0}(t)\sigma_{\rm G}^2 dM_0, \tag{35}$$

$$E_{\rm w}(t) = \int n(M_0)\frac{3}{2}W_{M_0}(t)(c_{\rm s}^2 + \sigma_{\rm G}^2)dM_0, \tag{36}$$

$$L_{\rm X}(t) = 2.2\cdot 10^{45}\left(\frac{M_{\rm g}^{\rm c}}{10^{14}M_\odot}\right)^2\left(\frac{R^{\rm c}}{1\ {\rm Mpc}}\right)^{-3} \times\left(\frac{T_{\rm g}}{1\ {\rm keV}}\right)^{0.3}\ {\rm erg\ s^{-1}}, \tag{37}$$

where $L_{\rm X}$ is the cooling rate (erg s^{-1}) due to the thermal bremsstrahlung without metals (Cox, Tucker 1969), $W_{M_0}(t)$ and $S_{M_0}(t)$ are the gas-ejection rates of a galaxy from the initial galaxy mass M_0 by the galactic wind and ram-pressure stripping, respectively, and $R^{\rm c}$ and $T_{\rm g}$ are the cluster radius and the temperature of the ICM, respectively. We should replace $c_{\rm s}^2$ with $c_{\rm s}^2 - v_{\rm escape}^2$ for a specific energy of the ejected gas. Since our galaxy model is one-zone, $v_{\rm escape}$ should be the averaged value. In spite of overestimating for heating by the galactic wind, the effect is negligible even if we take $v_{\rm escape} = 0$, because the velocity disperson of galaxies is much greater than the sound velocity.

Since a cluster is assumed to be a closed system, the total mass of galaxies and the ICM is constant. By assuming that galaxies and ICM are in the gravitational equilibrium, it is given by

$$\left[\frac{M_{\rm G}^{\rm c}(t) + M_{\rm g}^{\rm c}(t)}{10^{13}\ M_\odot}\right] = 11.6\ k_m\left(\frac{R^{\rm c}}{1\ {\rm Mpc}}\right)\left[\frac{T_{\rm g}(0)}{1\ {\rm keV}}\right], \tag{38}$$

where k_m is the ratio of the total mass of galaxies and the ICM to the virial mass. Therefore, $k_m = 1$ means that no dark matter exists and $k_m = 0$ means that dark matter exists only in a cluster.

We take 1 Mpc as the cluster radius, $R^{\rm c}$. The reasons are as follows: Since we assume the one-zone model for the cluster of galaxies for simplicity, and the density is homogeneous everywhere, the ram-pressure stripping at the central region is underestimated. Therefore, we should take a smaller value as the cluster radius to estimate the stripping effect correctly. On the other hand, if we take a much smaller radius than the observational one, it is hard to compare our model with the observed metallicity, because that metallicity is the mean value within the observed region, not the value in the central region. Thus, we take 1 Mpc as the cluster radius from these two competitive conditions.

Table 5. Model W for X-ray clusters.

Model	α $(10\ \mathrm{Gyr})^{-1}$	μ	t_w (Gyr)	M_G^c $(10^{13}M_\odot)$	M_g^c $(10^{13}M_\odot)$	M_{Fe}^c $(10^{10}M_\odot)$	M_g^c/M_G^c	Z_{Fe}^c $(Z_{Fe_\odot})$	L_X $(10^{45}\ \mathrm{erg\ s^{-1}})$	T_g (keV)
IC	...	...	...	7.2	7.2	0	1.0	0	0.84	6.2
Wa	30	0.85	0.5	2.8	12	7.8	4.2	0.41	1.6	3.1
Wb	30	1.35	1.0	6.5	7.9	2.6	1.2	0.20	0.98	3.5
Wc	100	0.85	0.1	4.1	10	16	2.5	0.92	1.6	3.2
Wd	100	1.35	0.5	6.8	7.7	1.8	1.1	0.14	0.93	3.6
We	100	1.35	1.0	6.9	7.5	0.68	1.1	0.055	0.91	3.6
Wf	300	1.35	0.5	6.9	7.6	0.77	1.1	0.062	0.91	3.6

Table 6. Model WS for X-ray clusters.

Model	α $(10\ \mathrm{Gyr})^{-1}$	μ	t_w (Gyr)	M_G^c $(10^{13}M_\odot)$	M_g^c $(10^{13}M_\odot)$	M_{Fe}^c $(10^{10}M_\odot)$	M_g^c/M_G^c	Z_{Fe}^c $(Z_{Fe_\odot})$	L_X $(10^{45}\ \mathrm{erg\ s^{-1}})$	T_g (keV)
IC	...	...	...	7.2	7.2	0	1.0	0	0.84	6.2
WSa	30	0.85	0.5	2.5	12	7.9	4.7	0.41	1.6	3.1
WSb	30	1.35	1.0	6.4	8.0	2.7	1.3	0.20	1.0	3.5
WSc	100	0.85	0.1	3.9	11	16	2.7	0.92	1.6	3.2
WSd	100	1.35	0.5	6.5	7.9	3.0	1.2	0.23	0.98	3.5
WSe	100	1.35	1.0	6.5	7.9	2.9	1.2	0.23	0.98	3.5
WSf	300	1.35	0.5	6.6	7.9	3.7	1.2	0.28	0.97	3.5

5. Numerical Results for X-Ray Clusters of Galaxies

5.1. *Observational Constraints*

Several quantities, such as the mass, temperature, and iron abundance of the ICM and X-ray fluxes for rich clusters of galaxies, are tabulated in Arnaud et al. (1992) and Tsuru (1992) based on the X-ray satellite observations. For reference, we summarize eight clusters of galaxies including Virgo, Perseus (A426), and Coma (A1656) in table 4 from their results. The columns in table 4 are the cluster name, the galaxy mass, M_G^c, the ICM mass, M_g^c, the iron mass in the ICM, M_{Fe}^c, the mass ratio of the ICM to the galaxy, M_g^c/M_G^c, the iron abundance in the ICM, Z_{Fe}^c, the X-ray luminosity at 2–10 keV, L_X, and the temperature of the ICM, T_g.

Since they estimated the quantities of X-ray clusters assuming the cluster radius to be 3 Mpc, we recalculated the galaxy mass within $R^c = 1$ Mpc by using observations by Arnaud et al. (1992) as follows. At first, we estimated the galaxy mass at $R^c = 3$ Mpc by using the mass-to-luminosity ratio and V-band luminosity for spirals, lenticulars, and ellipticals in Arnaud et al. (1992), assuming that the mass-to-luminosity ratio is the same for both spirals and lenticulars. Although we underestimated the galaxy mass because the mass-to-luminosity ratio for lenticulars is slightly larger than that of spirals, the difference is around 10% of the galaxy mass. If we take the King model for the galaxy distribution in a cluster,

$$\frac{\rho_G(R^c)}{\rho_G(0)} = [1 + (R^c/a)^2]^{-3/2}, \tag{39}$$

where ρ_G and a are the galaxy density and the core radius of the galaxy distribution, respectively, we can finally obtain the galaxy mass at $R^c = 1$ Mpc by using the relation $M_G^c(1\ \mathrm{Mpc})/M_G^c(3\ \mathrm{Mpc}) = 0.52$ from the above equation with $a = 0.25$ Mpc (Sarazin 1986).

We adopt the so-called β-model in order to determine the mass of the ICM. The ICM distribution is given by

$$\frac{\rho_c(R^c)}{\rho_c(0)} = [1 + (R^c/a)^2]^{-3\beta/2}, \tag{40}$$

where β is the square of the ratio of the velocity dispersion of galaxies to the isothermal sound speed of the ICM. We estimate the ICM mass at $R^c = 1$ Mpc using the relation $M_g^c(1\ \mathrm{Mpc})/M_g^c(3\ \mathrm{Mpc}) = 0.25$, obtained from the above equation with $\beta = 2/3$ (Jones, Forman 1984; Fukumoto, Ikeuchi 1992). In this case, the ICM distribution depends on r^{-2} at far away.

We did not take account of the abundance of α-elements (Mg, O, Ne, Si, S, ...) in the constraints to the model. The reasons were as follows: Worthey et al. (1992) found that Mg is overabundant with respect to Fe when compared to the solar value. Since [Mg/Fe] is from 0.2 to 0.3 in giant elliptical galaxies, it is highly probable that the main contributors to the Fe enrichment of the interstellar gas are the type II SNe. Thus, we do not deny the possibility that our model is not consistent with the observations. However, it is not clear how many α-elements are theoretically produced in a type II SN. Moreover, in the four clusters of galaxies, the observed metallicities of α-elements are not sufficiently accurate to conclude that the type II SNe contribute to the Fe enrichment of the ICM, because the 90% confidence errors are very large (Mushotzky 1994). Our goal was to investigate the effects of the stripping to the ICM abundance by the ram pressure of the intracluster gas. Therefore, we did not make use of the α-elements as constraints to the present model.

5.2. *Dependence on Elliptical Models*

Adopted parameters are $(\alpha, \mu, k, f_{\rm SNI})$=(1.0,1.35,1,0.1) for spirals, and six sets of parameters for ellipticals are summarized in table 3. In the case when we ignore the gas stripping from ellipticals, i.e., only the galactic wind is included, the numerical results are presented in table 5, and is called the model W. In the case when both the galactic wind and gas stripping are considered, the results are presented in table 6, and is called the model WS. The columns in tables 5 and 6 are as follows: The 1st column is the model name, and from the 2nd to 4th columns are the adopted parameters as the star-formation coefficient, α, the power index of the IMF, μ, and the time when galactic wind occurs, $t_{\rm w}$. From the 5th to 10th are the calculated results at $t = 15$ Gyr as the galaxy mass, $M_{\rm G}^{\rm c}$, the ICM mass, $M_{\rm g}^{\rm c}$, the iron mass in the ICM, $M_{\rm Fe}^{\rm c}$, the iron abundance in the ICM, $Z_{\rm Fe}^{\rm c}$, the X-ray luminosity at 2–10 keV, L_X, and the temperature of the ICM, $T_{\rm g}$. Other adopted parameters are as follows: $M_{\rm g}^{\rm c}(0)/M_{\rm G}^{\rm c}(0) = 1$, $k_m = 0.2$, $\gamma = 0.1$ for spirals, and $\gamma = 1.0$ for ellipticals, and $\sigma_{\rm G} = 1000$ km s^{-1}. Model IC in tables 5 and 6 are the initial state of a cluster of galaxies.

As can be seen in these tables, the iron abundances are more than 0.4 solar values for four models Wa, Wc, WSa, and WSc. (We hereafter call the model a for Wa and WSa altogether.) These seem to be too large compared with the observations. Other models show less iron abundances than 0.2 solar values, the same or smaller than the observations. The reasons are as follows: For models a, b, and c, both the iron abundance and the ejected gas mass are larger, because the star-formation rate is small and/or the initial-mass function is gentle compared with that of other models. For models d, e, and f, the iron abundances of the model WS are 2–4 times larger than those of the model W. In order to see the reason, we summarize the epoch when the gas is released from galaxies in table 7. The columns in table 7 are the model name, the galactic-wind epoch and the gas stripping epoch for ellipticals, and that for spirals with $M_{\rm G} = 5 \times 10^{10}\ M_\odot$. The cases with the bracket (WSa, WSb, WSc) in the 3rd column indicate that the stripping occurs after the galactic wind blows. Since most of the interstellar gas is ejected by the galactic wind, the results are the same as in the case of no gas stripping, i.e., model W, as is seen in tables 5 and 6. On the other hand, gas stripping occurs before the galactic wind blows in three models WSd, WSe, and WSf. In these cases most of the interstellar gas is lost by the gas stripping slightly earlier than in model W. As can be seen in figures 2b and 2c, since the iron mass in interstellar gas is maximum slightly earlier than 0.5 Gyr, the ejected iron masses in these three cases are much larger than in the corresponding cases of model W.

Table 7. Gas release epochs.

Model	Ellipticals		Spirals ($5 \cdot 10^{10} M_\odot$)
	$t_{\rm w}$ (Gyr)	$t_{\rm s}$ (Gyr)	$t_{\rm s}$ (Gyr)
WSa	0.5	(2.2)	9.8
WSb	1.0	(1.2)	12.8
WSc	0.1	(0.62)	9.4
WSd	0.5	0.36	12.8
WSe	1.0	0.36	13.0
WSf	0.5	0.11	13.0

In model c, the iron abundance of ICM is much larger than the observed values (see table 4). We must assume that the mass ratio of the primordial gas to the initial galaxies, $M_{\rm g}^{\rm c}(0)/M_{\rm G}^{\rm c}(0)$, is larger than unity in order to account for the observed iron abundance. However, the mass ratio of the ICM to member galaxies, $M_{\rm g}^{\rm c}/M_{\rm G}^{\rm c}$, increases with the cluster richness, contrary to observations. Therefore, model c is not suitable for a cluster of galaxies. On the other hand, in models d, e, and f the iron abundance of the ICM is too small compared with the observations. Therefore, it seems that the intermediate model between models a and b presents a good agreement with the observations. This means that gas stripping is not important, although the possibility that it contributes to the ICM can not be denied.

We simply estimate the ejected gas mass and its iron abundance by using two observations, the mass ratio of the ICM to member galaxies, $M_{\rm g}^{\rm c}/M_{\rm G}^{\rm c}$, and the iron abundance of the ICM, $M_{\rm Fe}^{\rm c}/M_{\rm g}^{\rm c}$. If it is assumed that the mass of the primordial gas, $M_{\rm g}^{\rm c}(0)$, is the same as that of

Table 8. Fraction of spirals experiencing the gas stripping of the model WSd.

Redshift	t (Gyr)	f_s	f_B
1.4.....	5.4	0.57	...
0.5.....	9.6	0.63	0.25
0.2.....	13	0.68	0.10
0.0.....	15	0.72	0.03

initial member galaxies, $M_G^c(0)$, we can obtain these two quantities as

$$\frac{M_g^c}{M_G^c} = \frac{1+x}{1-x}, \tag{41}$$

and

$$\frac{M_{Fe}^c}{M_g^c} = \frac{xy}{1+x}, \tag{42}$$

where $x = \Delta/M_g^c(0)$ and $y = M_{Fe}^c/\Delta$, Δ being the total gas mass released from the member galaxies. From observations, we take $M_g^c/M_G^c = 2$ and $M_{Fe}^c/M_g^c = 0.3\ Z_{Fe_\odot}$. As a result, it is obtained that $x = 1/3$ and $y = 1.2\ Z_{Fe_\odot}$. Therefore, one-third of the total mass of member galaxies are released into the intracluster space. For models in tables 5 and 6 of $M_G^c(0) = M_g^c(0) = 7.2 \times 10^{13} M_\odot$, $x = 1/3$ corresponds to $M_G^c = 4.8 \times 10^{13} M_\odot$ and $M_g^c = 9.6 \times 10^{13} M_\odot$. The average iron abundance of the released gas, Z_{Fe}^E, is $1.2\ Z_{Fe_\odot}$. As shown in table 3, the ejected iron abundances, Z_{Fe}^E, from ellipticals are much larger than $1.2\ Z_{Fe_\odot}$ in all models. Nevertheless, the resultant iron abundances of the ICM are smaller than $0.3\ Z_{Fe_\odot}$ in models Wb, Wd, We, and Wf. This suggests that metal-poor gas is released from spirals by ram-pressure stripping.

In any models the temperature of the ICM (almost 3.5 keV) is lower than that of observations by a factor of 2, because we did not take account of the ICM heatings by the release of gravitational energy due to gas infall within the cluster and by the thermalization of random motions of galaxies. Moreover, even if the galaxy mass is $10^{12} M_\odot$, c_s is around 230 km s^{-1}. Thus, the galactic wind does not heat up the ICM because of $c_s^2 < \sigma_G^2$ as in equation (36).

In the model WS, a part of spirals experience the ram-pressure stripping. As described in subsection 2.2.1, a less massive spiral is much more stripped by the ram pressure. Their critical masses are $5 \times 10^{10} M_\odot$ in models WSb, WSd, WSe, and WSf, and $7 \times 10^{10} M_\odot$ in models WSa and WSc, because the amount of the ICM ejected from ellipticals in the latter is larger than that in the former. Thus, as can be seen in table 7 for the same spiral mass, gas stripping occurs during an earlier epoch in the latter. We simply estimate the evolution of the fraction f_s of spirals which suffer gas stripping by using the relation between the spiral mass and its stripping epoch. The columns in table 8 are the redshift, the time corresponding to its redshift (assuming Hubble constant H_0=50 km s^{-1} Mpc^{-1} and $q_0 = 0.1$), and f_s. In addition, we present f_B the fraction of galaxies whose rest-frame $B-V$ colors are, at least, 0.2 mag bluer than that at the peak in number of early type galaxies (Butcher, Oemler 1984). If stripped spirals grow redder, the fraction f_B would decrease. Since f_B decreases much faster than $(1-f_s)$, the so-called the Butcher-Oemler effect seems to come from the intrinsic evolution of galaxies rather than their environmental effect, as pointed out by them.

5.3. *Dependence on the Parameters of Ellipticals*

The dependence of results on three parameters (α, μ, t_w) in ellipticals is summarized in table 9. The center of the parameter space of the three parameters is in the WSd model, as shown in the first row. The columns in table 9 are as follows: From the 1st to 3rd columns are the adopted parameters as the star-formation coefficient, α, the power index of the IMF, μ, and the time when galactic wind blows, t_w. From the 4th to 10th are the calculated results at $t = 15$ Gyr as the galaxy mass, M_G^c, the ICM mass, M_g^c, the iron mass in the ICM, M_{Fe}^c, the iron abundance in the ICM, Z_{Fe}^c, the X-ray luminosity at 2–10 keV, L_X, and the temperature of the ICM, T_g. As described in subsection 3.2, $k = 1$ is fixed because the resultant evolutionary behaviors in varying k are essentially the same as that in varying α. Other parameters, $M_g^c(0)/M_G^c(0)$, k_m, and γ are the same as in tables 5 and 6.

From table 9, only the iron abundance depends strongly on the power index of the IMF, though the iron abundance in galaxies depends on the star-formation rate as well as the power index of the IMF. The iron abundances in the case $\alpha = 300$ and the case $t_w = 1$ Gyr are almost the same as that of the case $\alpha = 100$, because gas stripping occurs before the galactic wind for these cases. We note that the galactic wind blows earlier with decreasing the power index of the IMF. The released iron mass decreases for the late wind, and increases for the early wind.

5.4. *Dependence on Parameters of a Cluster*

The dependence of the results on the two parameters of the cluster type, the number ratio of ellipticals to spirals, N_E/N_S, and the velocity dispersion, σ_G, is summarized in table 10. The columns in table 10 are as follows: The 1st and 2nd columns are the number ratio of ellipticals to spirals, N_E/N_S, and the velocity dispersion, σ_G. From the 3rd to 9th are the calculated results at $t = 15$ Gyr as the galaxy mass, M_G^c, the ICM mass, M_g^c, the iron mass in the ICM, M_{Fe}^c, the iron abundance in the ICM, Z_{Fe}^c, the X-ray luminosity at 2–10 keV, L_X, and the temperature

Table 9. Model WS for X-ray clusters with varying parameters for ellipticals.

α $(10\ \mathrm{Gyr})^{-1}$	μ	t_w (Gyr)	M_G^c $(10^{13}M_\odot)$	M_g^c $(10^{13}M_\odot)$	M_{Fe}^c $(10^{10}M_\odot)$	M_g^c/M_G^c	Z_{Fe}^c $(Z_{Fe_\odot})$	L_X $(10^{45}\ \mathrm{erg\ s^{-1}})$	T_g (keV)
100	1.35	0.5	6.5	7.9	3.0	1.2	0.23	0.98	3.5
30	1.35	0.5	5.5	8.9	4.6	1.6	0.32	1.2	3.3
300	1.35	0.5	6.6	7.9	3.7	1.2	0.28	0.97	3.5
100	0.85	0.5	5.9	8.6	11	1.5	0.75	1.1	3.5
100	1.85	0.5	6.8	7.6	0.75	1.1	0.060	0.92	3.5
100	1.35	0.1	5.2	9.2	5.6	1.8	0.37	1.2	3.2
100	1.35	1.0	6.5	7.9	2.9	1.2	0.23	0.98	3.5
100	1.35	No	6.8	7.7	2.6	1.1	0.21	0.92	3.5

Table 10. Dependence on cluster types of X-ray clusters.

N_E/N_S	σ_G (100 km s^{-1})	M_G^c $(10^{13}M_\odot)$	M_g^c $(10^{13}M_\odot)$	M_{Fe}^c $(10^{10}M_\odot)$	M_g^c/M_G^c	Z_{Fe}^c $(Z_{Fe_\odot})$	L_X $(10^{45}\ \mathrm{erg\ s^{-1}})$	T_g (keV)
0	8	4.5	4.7	0.11	1.0	0.015	0.26	2.6
0	10	6.7	7.7	0.39	1.2	0.030	0.95	3.6
0	12	8.5	12	1.3	1.4	0.067	2.7	4.3
1.0	8	4.3	4.9	1.2	1.1	0.15	0.29	2.6
1.0	10	6.5	7.9	3.0	1.2	0.23	0.98	3.5
1.0	12	8.8	12	6.2	1.4	0.32	2.6	4.2
∞*	8	4.2	5.0	1.6	1.2	0.19	0.29	2.6
∞	10	6.5	8.0	3.8	1.2	0.29	0.99	3.5
∞	12	8.9	12	7.8	1.3	0.40	2.5	4.2

* This means no spiral galaxy.

of the ICM, T_g.

Since the initial gas mass of the ICM is taken as $7.2\times10^{13}M_\odot$, from table 10, the released gas mass is $0.8\times10^{13}M_\odot$ in the case that all galaxies are ellipticals, $N_E/N_S = \infty$, and $0.5\times10^{13}M_\odot$ for only spirals, $N_E/N_S = 0$ for the case of $\sigma = 1000$ km s^{-1}. Thus, the contribution to the gas mass of ellipticals is, at most, twice that of spirals. However, the contribution to the ICM from galaxies is much smaller than the primordial gas. Furthermore, since the iron mass released from ellipticals is around ten-times that of spirals, the contribution of ellipticals to the iron abundance is much larger than that of spirals. These two results indicate that the iron abundance of the gas ejected from ellipticals is several-times large compared with spirals. Arnaud et al. (1992) pointed out in their figure 2 that there seems no correlation between total spiral luminosities and the gas mass. As can be seen in the above, since the gas released from spirals per unit luminosity is not so much different from that from ellipticals, this result can be understood by the observational tendency that the spiral fraction decreases with increasing the richness of clusters (Arnaud et al. 1992, see table 2). In fact, in their figure 2 there seems to exist a clear correlation with a larger slope than 1.9. This suggests that the spiral fraction decreases with increasing the gas mass, because the increase rate of spiral luminosities with increasing the gas mass is much smaller than that of the total luminosities. However, it is not clearly concluded that the spiral fraction really decreases with increasing the richness of a cluster of galaxies, because Andreon (1993) showed that the correlation between the cluster richness and the spiral fraction might be an observational bias by using the X-ray luminosity and spiral fraction of nearby clusters of galaxies.

As can be seen in table 4, the iron abundance of the ICM is nearly constant, or decreases, with increasing the

temperature or the velocity dispersion of galaxies. These results are contrary to the observations. In our model, the ram pressure of the ICM becomes larger with increasing the velocity dispersion of galaxies, so that the gas release epoch becomes earlier in ellipticals and the upper mass of spirals which suffer the ram-pressure stripping increases. Finally, the gas mass and the iron mass released from both types of galaxies increase. Even if the spiral fraction decreases with increasing the velocity dispersion of galaxies, this tendency does not change, because the iron mass is essentially proportional to the mass fraction of ellipticals. There are two possibilities for reducing this discrepancy. One is that the elliptical model taken in our calculation is wrong for clusters of galaxies. However, if the model with a small power index of the IMF is adopted in rich clusters, the mass ratio of the ICM to galaxies cannot be reproduced, though the iron abundance is in agreement with observations. The other is that the mass ratio of the primordial gas to galaxies is large with increasing the temperature or the velocity dispersion of galaxies. This gives strong constraints on galaxy formation.

6. Summary

In this paper we investigated the thermal and chemical evolution of X-ray clusters of galaxies, pursuing the chemical evolution and gas ejection of member galaxies. To do so, at first, evolution models of spirals and ellipticals in the field were constructed. The spiral model consistent with observations is that the star-formation coefficient α (in units of 1/10 Gyr) is 1.0 and the power index μ of the IMF is 1.35 (Salpeter 1955) for the case that the star-formation rate is proportional to the interstellar gas mass, i.e., $k = 1$. (Even for the case $k = 1/2$ or 2, we find α which is in good agreement with observations.) In ellipticals, we adopted six models summarized in table 3; the ejected iron abundances are more than 1.5 times that of the solar abundance.

Based on the best model for spirals and six models for ellipticals, the evolutions of X-ray clusters of galaxies were calculated. In three cases of elliptical models, the epoch when the ram-pressure stripping by the ICM occurs is earlier than the galactic-wind epoch, so that the ejected iron mass and the iron abundance of the ICM increase. Butcher and Oemler (1984) showed that bluer spirals decrease with decreasing the redshift. Since from our results the fraction of spirals experiencing gas stripping increases much slower than the decreasing rate of bluer spirals, the Butcher-Oemler effect seems to arise due to the intrinsic evolution of spirals.

As for the parameters dependence of X-ray clusters of galaxies on ellipticals, the iron abundance of the ICM depends strongly on the initial-mass function, but not on the star-formation rate, and intermediately on the galactic-wind epoch and the cluster richness. Furthermore, the dependence on the number ratio of ellipticals to spirals indicates that though the contribution to the iron mass of the ICM from spirals is smaller than that from ellipticals, the ejected gas mass from spirals is the same as that from ellipticals. Thus, we can not ignore the contributions of spirals. Though the conclusion that the contribution to the ICM from galaxies is much smaller than the primordial gas had already been suggested by Matteucci and Vettolani (1988), David, Forman, and Jones (1991) and Arnaud et al. (1992), for the first time we showed this fact quantitatively by including spirals as well as ellipticals. On the other hand, the iron abundance of the ICM increases with increasing the galaxy velocity dispersion. To be in agreement with the observations, the mass ratio of the primordial gas to the member galaxies increases with increasing galaxy velocity dispersion. This puts strong constraints on the galaxy formation. This result has already derived by Arnaud et al. (1992). However we independently derived the same result using the thermal and chemical evolution model.

In this model we assume one-zone model for a cluster of galaxies. However, the observed intracluster gas density decreases from the center to the outer layer and the ram-pressure stripping in spirals occurs efficiently at the core. Further, radiative cooling is more effective in the core of cluster, so that a temperature gradient arises. To treat these effects exactly, we must consider the structure of a cluster in the future.

We would like to thank Dr. Takuji Tsujimoto and Professor Ken'ichi Nomoto for presenting the table of chemical-elements abundances ejected from type II SNe and for having kindly providing the Ph. D. Thesis of Dr. T. Tsujimoto. We would also like to thank Professor Nobuo Arimoto for very useful conversations. We are very grateful to colleagues at our institute for continuing encouragement. This work was supported in part by the Grant-in-Aid for Encouragement of Young Scientists by the Ministry of Education, Science, Sports and Culture of Japan (No. 3566).

Appendix. Symbols and Their Meanings

	Symbol		Meaning
Star	m		a stellar mass
	ϕ		initial-mass function (IMF)
	μ		power index of the IMF and μ=1.35 corresponds to Salpeter's
	τ_m		life time of a star with mass m
	$R(m)$		mass fraction released from a star with m
	$R_{\rm Fe}(m)$		iron fraction released from a star with m
	$f_{\rm SNI}$		fraction of binary systems
Galaxy	$t_{\rm w}$		galactic-wind epoch
	$M_{\rm s}$		stellar mass
	$M_{\rm g}$		interstellar gas mass
	$M_{\rm G}$	$= M_{\rm s} + M_{\rm g}$	the galaxy mass
	L_B		galaxy luminosity with B-band
	$M_{\rm total}$		total (virial) mass
	$M_{\rm Fe}$		iron mass contained in the intestellar gas
	$M_{\rm g}({\rm wind})$		interstellar gas mass at the galactic-wind epoch
	$M_{\rm g}^{\rm E}$		total ejected gas mass
	$M_{\rm Fe}^{\rm E}$		total ejected iron mass
	$Z_{\rm Fe}$	$= M_{\rm Fe}/M_{\rm g}$	the iron abundance in the interstellar gas
	$Z_{\rm Fe}^{\rm E}$	$= M_{\rm Fe}^{\rm E}/M_{\rm g}^{\rm E}$	the average iron abundance which is ejected into the intracluster space
	$R_{\rm G}$		galaxy radius
	$n_{\rm g}$		interstellar number density
	$\rho_{\rm g}$		interstellar gas density
	$c_{\rm s}$		sound velocity
	$\sigma_{\rm s}$		star's velocity dispersion
	$E_{\rm g}$		thermal energy
	γ		galaxy structure parameter
Cluster	$M_{\rm G}^{\rm c}$		member galaxy mass
	$M_{\rm g}^{\rm c}$		mass of the ICM
	$M_{\rm Fe}^{\rm c}$		iron mass contained in the ICM
	$Z_{\rm Fe}^{\rm c}$	$= M_{\rm Fe}^{\rm c}/M_{\rm g}^{\rm c}$	the iron abundance
	$R^{\rm c}$		cluster radius, which is fixed with 1 Mpc
	$\rho_{\rm c}$		ICM density
	$\sigma_{\rm G}$		galaxy's velocity dispersion
	$E_{\rm g}^{\rm c}$		thermal energy
	$T_{\rm g}$		temperature
	$L_{\rm X}$		X-ray luminosity
	$n(M_0)$		luminosity function of member galaxies
	k_m		ratio of the sum of the mass of member galaxies and the ICM to the virial mass
Rate	$F(t)$		star-formation rate
	α		star-formation coefficient
	k		power index of the star-formation rate
	$G(t)$		mass loss rate
	$G_{\rm Fe}(t)$		mass loss rate for the iron
	$W(t)$		galactic wind rate
	$S(t)$		ram-pressure stripping rate

References

Allen C.W. 1973, Astrophysical Quantities (Athlone, London) p31
Andreon S. 1993, A&A 276, L17
Arimoto N., Yoshii Y. 1986, A&A 164, 260
Arimoto N., Yoshii Y. 1987, A&A 173, 23
Arnaud M., Rothenflug R., Boulade O., Vigroux L., Vangioni-Flam E. 1992, A&A 254, 49
Binney J., Tremaine S. 1987, Galactic Dynamics (Princeton University Press, Princeton) p618
Butcher H., Oemler A. Jr 1984, ApJ 285, 426
Ciotti L., D'Ercole A., Pellegrini S., Renzini A. 1991, ApJ 376, 380
Cox D.P., Tucker W.H. 1969, ApJ 157, 1157
David L.P., Forman W., Jones C. 1990, ApJ 359, 29
David L.P., Forman W., Jones C. 1991, ApJ 380, 39
Dressler A., Lynden-Bell D., Burstein D., Davies R.L., Faber S.M., Terlevich R.J., Wegner G. 1987, ApJ 313, 42
Edge A.C., Stewart G.C. 1991a, MNRAS 252, 414
Edge A.C., Stewart G.C. 1991b, MNRAS 252, 428
Faber S.M., Gallagher J.S. 1979, ARA&A 17, 135
Forman W., Jones C., Tucker W. 1985, ApJ 293, 102
Fukumoto J., Ikeuchi S. 1992, PASJ 44, L235
Gallagher J.S., Faber S.M., Balick B. 1975, ApJ 202, 7
Giovanelli R., Haynes M.P. 1983, AJ 88, 881
Gunn J.E., Gott J.R. III 1972, ApJ 176, 1
Hatsukade I. 1989, Ph.D. Thesis, The University of Osaka
Hillebrandt W. 1982, A&A 110, L3
Hills J.C. 1980, ApJ 225, 986
Himmes A., Biermann P. 1980, A&A 86, 11
Hughes J.P., Yamashita K., Okumura Y., Tsunemi H., Matsuoka M. 1988, ApJ 327, 615
Ikeuchi S. 1977, Prog. Theor. Phys. 58, 1742
Jones C., Forman W. 1984, ApJ 276, 38
Köppen J., Arimoto N. 1991, A&AS 87, 109
Larson R.B. 1974, MNRAS 166, 585
Larson R.B., Tinsley B.M. 1978, ApJ 219, 46
Madore B.F. 1977, MNRAS 178, 1
Mathieu R.D. 1983, ApJL 267, L97
Matteucci F., Tornambé A. 1987, A&A 185, 51
Matteucci F., Vettolani G. 1988, A&A 202, 21
Murakami I., Ikeuchi S. 1994, ApJ 420, 68
Mushotzky R.F. 1994, in New Horizon of X-Ray Astronomy—First Results from ASCA, ed F. Makino, T. Ohashi (Universal Academy Press, Tokyo) p243
Nomoto K., Thielemann F.-K., Yokoi K. 1984, ApJ 286, 644
Pagel B.E.J., Edmunds M.G. 1981, ARA&A 19, 77
Renzini A., Ciotti L., D'Ercole A., Pellegrini S. 1993, ApJ 419, 52
Renzini A., Voli M. 1981, A&A 94, 175
Saito M. 1979, PASJ 31, 181
Salpeter E.E. 1955, ApJ 121, 161
Sandage A. 1990, in Clusters of Galaxies, ed W.R. Oegerle, M.J. Fitchett, L. Danly (Cambridge University Press, cambridge) p201
Sarazin C.L. 1986, Rev. Mod. Phys. 58, 1
Schmidt M. 1959, ApJ 129, 243
Sullivan W.T. III, Johnson P.E. 1978, ApJ 225, 751
Takahara F., Ikeuchi S. 1977, PASJ 58, 1728
Takeda H., Nulsen P.E.J., Fabian A.C. 1984, MNRAS 208, 261
Tammann G.A. 1974, in Supernovae and Supernova Remnants, ed C.B. Cosmovici (Reidel, Dordrecht) p155
Tinsley B.M. 1980, Fund. Cosm. Phys. 5, 287
Toyama K., Ikeuchi S. 1980, Prog. Theor. Phys. 64, 831
Trimble V. 1987, ARA&A 25, 425
Tsujimoto T. 1994, Ph.D. Thesis, The University of Tokyo
Tsuru T. 1992, Ph.D. Thesis, The University of Tokyo
Tully R.B., Fisher J.R. 1977, A&A 54, 661
Worthey G., Faber S.M., Gonzalez J.J. 1992, ApJ 398, 69
Young J.S., Scoville N.Z. 1991, ARA&A 29, 581